Lessons Learned in Developing Sensorised Textiles to Capture Body Shapes

Leonardo A. García-García[1(✉)], George Valsamakis[1], Niko Münzenrieder[1,2], and Daniel Roggen[1]

[1] Sensor Technology Research Centre, University of Sussex, Brighton BN1 9QT, UK
l.a.garcia-garcia@sussex.ac.uk

[2] Faculty of Science and Technology, Free University of Bozen-Bolzano, 39100 Bozen, Italy

Abstract. Motivated by the need to replace plaster casts or image acquisition approaches to capture body shapes to create orthoses, we explored the feasibility of using smart textile sleeve enhanced with arrays of stretch and bend sensors. The sensors' data is interpreted by an ad-hoc optimisation-based shape inference algorithm to come up with a digitised 3D model of the body part around which the sleeve is worn. This paper summarises the state of the art in the field, before illustrating the approach we followed and lesson's learned in developing smart textile sleeves and the associated data processing algorithms. The unique approach we followed was to realise from the ground up the sensing elements, their integration into a textile, and the associated data processing. In the process, we developed a technology to create stretch and bend sensing elements using carbon black and ecoflex, improving curvature detection; we also found ways to interconnect large arrays of such sensors, digitise their data, and developed several mathematical optimisation models for the inference of the sleeve shape from the sensor readings.

Keywords: Sensing sleeve · Smart textile · Body monitoring · Shape reconstruction · Flexible sensors

1 Introduction

New methods for the fabrication of personalised orthoses and prosthesis have been developed in recent years [7]. The increasing interest in developing personalised medical devices has prompted the application of technologies such as 3D printing or CNC machining to achieve this goal [1,15]. However, body acquisition systems has not advanced in the same pace, being 3D scanning [5,6] or photogrametric methods [1,7] the most used for creation of 3D models of the body. These systems can be faster, but they do not have a better accuracy or reliability than casting methods [5]. Therefore, new technologies such as smart textiles are required to obtain more accurate models of the body shape. The development of

H. Lewy and R. Barkan (Eds.): PH 2021, LNICST 431, pp. 365–380, 2022.
https://doi.org/10.1007/978-3-030-99194-4_23

flexible sensors has giving rise to the development of smart textiles with ubiquitous sensors for human motion monitoring [2,3,14], posture tracking [9], ECG signal analysis [16], or for shape measurement [8,12]. Despite of this, there is no register a functional textile to measure body shape.

Efforts for posture tracking includes optical fibre integrated in garments [4], inductive sensors for posture monitoring [9], stainless steel yarns [11], silicone with FBG sensors for lower back movement tracking [17]. Although the use of arrays stretchable sensors have been proposed [13,14], these have been limited to identify postures on the back.

The work here discussed is part of a project that focused on the development of a system for body shape sensing using a smart textile and a shape inference algorithm. The system aims to acquire body's shape to help in the fabrication of prostheses and orthoses. The device has been conceived as a smart textile enhanced with and array of bend/stretch sensors. The ends of each sensors is visualised as a node with coordinates in a $\mathbb{R}^3$ space. The coordinates of each node changes when the textile is worn, and this variation is proportional to the strain or bending angle of each sensor. A simulation of the sensors' array has been developed for the shape optimisation that includes a target and an inference meshes of n number of nodes that matches the number of the ends of the sensors, then gradient descent algorithm is used to optimise the inference shape to the target mesh. The system will help in the generation of accurate 3D models of the human body.

This paper presents the practical lessons learned during the ongoing work carried out to develop a smart sensing stretchable sleeve for body shape sensing. These lessons are here documented to show the progress and drawbacks made during the development with the intention to lead the way of those considering working on wearable technologies with similar characteristics. Section 2 presents a description of the system and shows the prototypes generated during the research, whil the algorithm used for the shape optimisation is presented in Sect. 3. Section 4 discusses issues presented during the development of the sleeve and the algorithm, finishing with the conclusions and future work in Sect. 6.

2 Shape Sensing Sleeve

The underlying principle of the shape reconstruction sleeve is the integration of flexible sensors in a stretchable textiles that will be able to measure localised changes in a stretchable textile as this goes from a rest state to a final stretched state. In this project this principle has been investigated with five different prototypes, each one with an array of sensors placed on a stretchable textile.

2.1 Stretchable Sleeve with Commercial Strain Sensors

The first iteration was formed by a commercial sleeve (Rymora Calf Compression Sleeves, Rymora Sports, UK) with 8 rings (Fig. 1); each ring had 8 commercial conductive rubber sensors of 20 mm length by 2 mm (Adafruit, USA). Firstly each sensor was connected to 0.19 mm enamelled copper wires on each end using conductive epoxy (CW2400, CircuitWorks, Chemtronics, Netherlands). The rings where then formed by attaching 8 sensors to an acrylic fettuccina yarn (Yeoman Yarns, Leicester, UK) with mouldable glue (Sugru, U.K.) separated 5 mm from each other. This resulted in non-stretchable sections of 16.12 $\pm$ 1.32 mm between each sensor. The rings where then placed on the sleeve 13.80 $\pm$ 1.55 mm apart from each other using adhesive and sewing the rigid areas to the sleeve. The array was connected to an interface software formed by four multi channel analogue multiplexers (CD74HC4067) plugged to an Arduino Uno board and the data was interface to the PC with MATLAB for data acquisition.

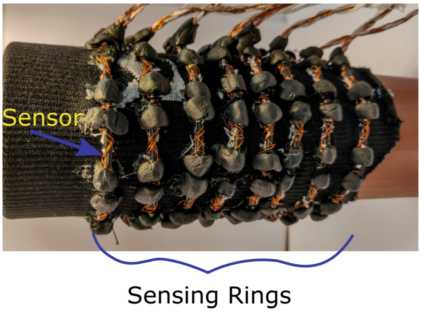

Fig. 1. Sensing sleeve with off-the-shelf sensors. The sensing sleeve is formed by 64 sensors arranged in 8 rings of 8 sensors each one.

2.2 Stretchable Sleeve with a Single Ring and Conductive Elastomer Strain and Bend Sensors

A second prototype was formed by a in house designed and fabricated stretchable sensors attached to a sleeve. This sensing device had a single ring formed with stretch and bend sensors made of Conductive Elastomer (CE). The composite material was created with silicone elastomer Ecoflex (00-30 Smooth-on, Pennsylvania, United States), Carbon Black (CB) (Vulcan P, Cabot, Boston, Massachusetts, United States), and heptane. Theses components were mixed with in the following ratios, 10 : 1.3 : 8. CB and heptane were mixed using a magnetic stirrer for 0.5 h, then Ecoflex part B was added and stirred for 5 h and Ecoflex part A was added and stirred for further 0.25 h. The solution was then degassed to remove all the air trapped during the mixing process and poured in 3D printed moulds. The 3D printed moulds were 20 mm long by 5 mm width by 2 mm thick. Each mould was prepared with fetuchina yarn to join the sensors. To prevent the material for the bend sensors from stretching, an extra piece of fetuchina yarn was added. Enamelled copper wires (0.19 mm) were placed on each end of each mould once the solution was poured to create the interfacing contacts for the sensors.

2.3 Stretchable Sleeve with a Single Ring and CE Strain and Bend Sensors Interfaced with Filament Wires

The third iteration was the same as the second prototype described in Sect. 2.2, but this time the copper wires for contacting the sensors were substituted for filament wires. The substitution was done enhance the interfacing, preventing the loosing of the contacts after stretching the sensors. Filament wires were selected after load and cyclic load test performed to CE interfaced with 5 different contacting methods [10].

2.4 Sleeve with a Long Array of CE Sensors and Filament Wires

A fourth prototype was build by designing an array of 70 CE sensors. The sensors are made of carbon black conductive nano particles embedded in a Ecoflex silicone matrix, and the fabrication process is the same as the one described in Sect. 2.2. A 3D printed mould was specially designed to generate four long stripes of sensors that will become four rings. The rings are connected to each other by a row of bend sensors. Each ring is comprised by a long stripe of five stretch alternated with five bent sensors connected in series, i.e. two sensors share a single interface. This reduced the number of interfacing wires to number of sensors $(n)+1$. The formed rings will measure changes in the perimeter of the cross section of the shapes where the sleeve is put on. The rings were joint with 3 rows of 10 inter-rings bend sensors connected in parallel to measure changes perpendicular to the cross section; each end of these sensors was interfaced with filament wire (Fig. 2). The sensors are 1.5 mm thick and 5 mm with lengths of 16 mm for bending sensors and 13 mm for strain sensors. The sensors are formed by the same mixture, and although the stretch sensors is only the piezoresistive material, the bend sensors were formed using two pieces of jute twine string fibre with the sensors' length which are covered in ecoflex and placed at the bottom of the moulds. This resulted in a thin layer of the piezoresistive material covering the surface which will generate changes in resistance proportional only to bending and not when stretching.

2.5 Sleeve with a Long Array of CE Sensors and Conductive Thread

The last prototype was created following the same process and configuration as the fourth prototype (Sect. 2.4), but the interfacing of the sensors was done using nylon thread coated with silver. This was used as textiles had demonstrated higher adhesion force to ecoflex [10]. This method improved the interfacing, resulting in less change in resistance due to the interfacing of the contacts. A data acquisition board was specially designed to acquire the data from the fourth and fifth prototype. The sleeve was interfaced to a PCB (Fig. 3) that has 6 circuits connected to a microcontroller system (Teensy 3.2). The measurements from the rings are acquired by four circuits with two 16 channel analogue multiplexers, two Op Amp, and a digital potentiometer. The values of the bend sensors

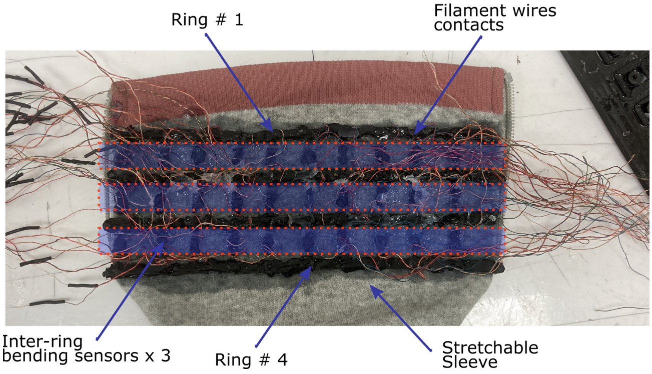

Fig. 2. Long array sleeve. The sensing sleeve is formed by 70 sensors arranged in 4 rings of 10 sensors each one and interconnected through three rows of bending sensors. The sensors in this prototype have been interfaced with filament wires.

connecting the rings are read by two circuits built with two 16 channels analogue multiplexers, one digital potentiometer, and one Op Amp. The multiplexer alternates each sensor to form a voltage divider with the digital potentiometer, which adjusts its value to the sensor resistance values for accurate results. The microcontroller is interfaced over a USB serial line. The data is acquired, stored, and processed in MATLAB.

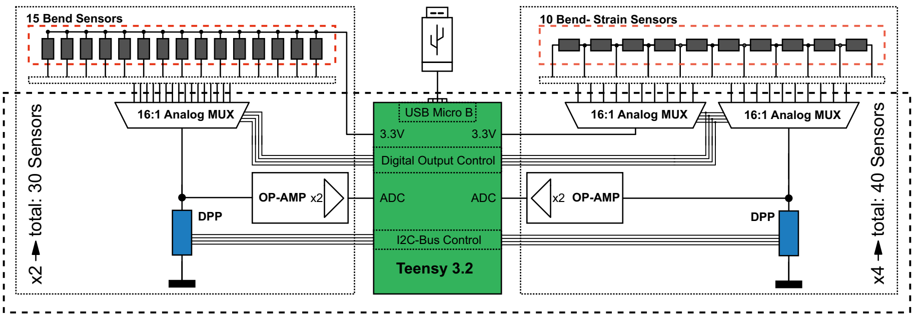

Fig. 3. Read out circuit. Made of 6 individual circuits: two 16 channels analogue multiplexers, 1 digital potentiometer, and 2 Op Amps to read the data from each ring. The other 2 circuits read data from 30 inter-ring bend sensors using a 16 channel analogue multiplexer, 1 digital potentiometer, and 2 Op Amps.

3 Shape Reconstruction

The sleeve sensor data is processed to infer the shape it is worn on (target shape) using the differences between sensors at rest and when conformed to an arbitrary shape. We used the reconstruction and simulations to explore the challenges in inferring the target shape given no prior knowledge other than the sleeve structure and sensors' readings. The number of sensors per ring, sensors reading accuracy and the errors, adds complexity to this challenge. The simulation is used to evaluate the reconstruction with higher number of sensors, different parameters and possibilities for error correction. A virtual model was developed and simulated to evaluate this process. The model is used to simulate draping over target shapes with varied morphology features and retrieve simulated sensor readings. The optimisation algorithm developed infers the target shape using only these measurements.

At first, simple target shapes were used, cylinders and cones. In the first approach using this algorithm [12], conical shapes were measured using the first iteration of the sleeve using only stretch sensors. Afterwards, we expanded the concepts further [8] to incorporate reading of bend sensor in the optimisation algorithm on shapes with arbitrary features such as curves, cross section twists, and lumps. In the latter, weighting factors for the reading of the bend sensor were incorporated and analysed, showing that certain target shapes benefited by adjusting these factors.

3.1 Reconstruction and Simulation Approach

The approach taken for the real and the simulated virtual sleeve is shown in Fig. 4. The steps for draping the virtual sleeve on STL models introduced the challenge to reproduce the way the physical sleeve is worn on a shape. This is because the level of detail in the reconstruction is limited by the number of sensors on the sleeve. This is important for the comparison of the end low-resolution result with the high-resolution STL model or real body limb.

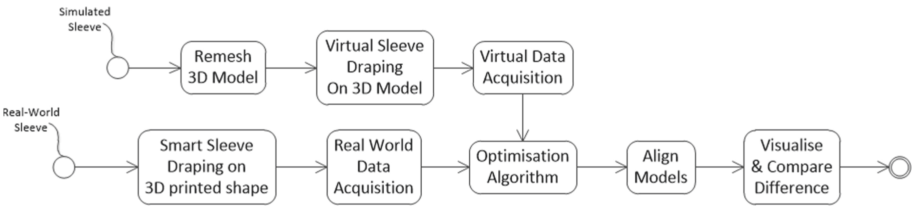

Fig. 4. Inference and simulation process.

While in the simulation the target shape is generated using a STL file, in the experimental part the sensors' data is passed to the optimisation function, producing the final set of points representing the target shape. From the optimisation stage onward, the process is common for both versions of the sleeve

3.2 Simulation Methodology

The following steps are followed to perform simulations:

1. Remesh and import target shape: The target shape is imported as a point cloud (Fig. 5).
2. Alignment and scaling: The target sleeve starts as a set of points of a cylindrical shape at a scale larger than the target shape. It is then centered to the centre of mass of the target shape and scaled.
3. Drape target sleeve over target shape: Using a number of estimation methods to adhere to the real sleeve constraints.
4. Optimise: Run minimisation algorithm to obtain an inferred sleeve that best matches the elongations and bends of the target sleeve.
5. Align and compare: Compare node Euclidean differences of the inferred sleeve vs. the target sleeve for evaluation.

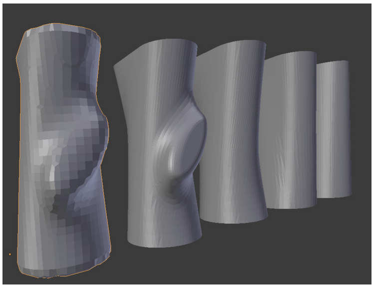

Fig. 5. Target shapes, remesh pre-processing for simulation.

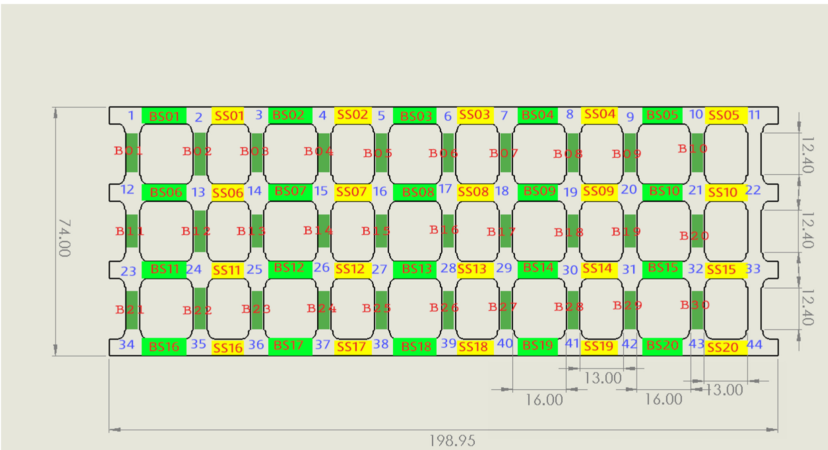

Fig. 6. Sleeve sensor structure. Bend Sensors (B and BS) in Green, Stretch sensors (SS) in yellow. (Color figure online)

The simulated model of the sleeve follows the sensor structure of the latest version of the sleeve, shown in Fig. 6. Figure 7 shows the initial, cylindrical state of the virtual sleeve, with the different edges coloured by type of sensor.

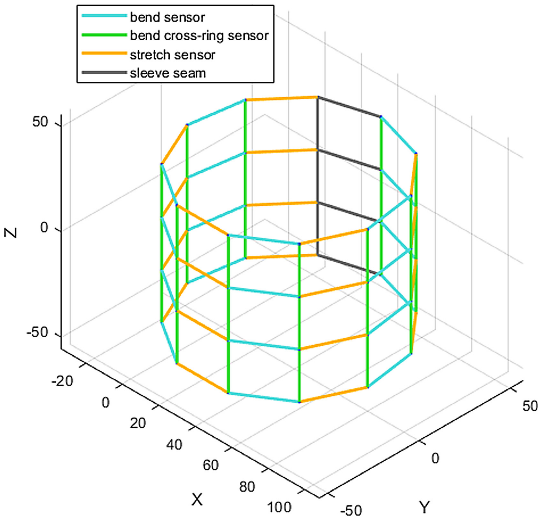

Fig. 7. Virtual sleeve in it's initial state.

3.3 Virtual Sleeve Alignment and Draping

This task moves points of the target sleeve from it's cylindrical form to points on the surface of the target shape. It is here referred to as conforming to shape or draping. The 2 geometries differ in the number of nodes that represent them so this is an $n \times m$ nodes task. The first objective is to align the 2 geometries, scale the target sleeve around the shape and translate to where required to cover the shape. Then, each node of the sleeve is moved to it's closest point of the shape. This process is filtered to conform to some of the constraints of the real sleeve. Figure 8 shows a 8 ring by 11 node sleeve draping over a bend shape. The corrections shown in red are examples of nodes that exceeded the maximum length between the rings.

Several other methods exist for performing this that can be explored: Iterative Closest Point, using geodesic distance instead of euclidean or using covariant distances. Other heuristics such as comparing surface normals for sets of points to detect curves could be used to improve results.

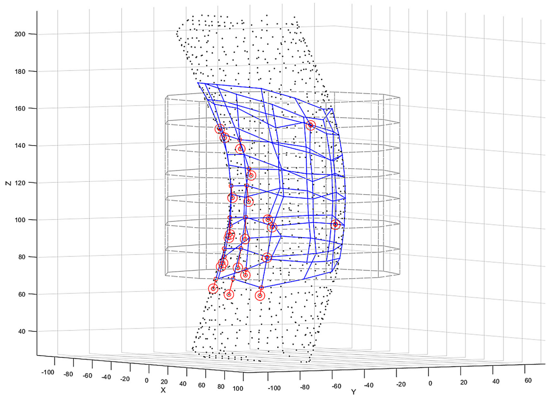

Fig. 8. An 8 by 11 sensor virtual ring (blue) draping over a bending shape (black point cloud). Outliar corrections are shown in red. (Color figure online)

3.4 Shape Inference Algorithm

This stage is oblivious to the shape and it attempts to converge a new sleeve geometry into the target sleeve by using the sensor measurements. The inference is carried out using an optimisation process based on the difference between the data obtained from the sensors when at rest and when they are in an active state (stretch or bend). The following equation that, derived in [8] is being used:

$$\begin{aligned} L = \sum_{i=1}^{E} \Bigg(\bigg(\left(e_{inf,i} - e_{tar,i}\right)^2 \cdot \lambda_1 \bigg) \\ + (1-\lambda_1) \cdot \Bigg(\bigg(\left(\theta_{\boldsymbol{C}_{inf},i} - \theta_{\boldsymbol{C}_{tar},i}\right)^2 \cdot \lambda_2 \bigg) \\ + \bigg(\left(\theta_{\boldsymbol{L}_{tar},i} - \theta_{\boldsymbol{L}_{inf},i}\right)^2 \cdot (1-\lambda_2) \bigg) \Bigg) \end{aligned}$$

Two weighting factors were introduced, $0 < \lambda_1 < 1$ and $0 < \lambda_2 < 1$. λ_1 assigns a higher importance to the matching lengths between the inferred shape and the sensor readings and a lower importance $(1 - \lambda_1)$ to the matching angles on the cross section; λ_2 assigns a higher importance to the angles on the cross section and the remaining value $(1 - \lambda_2)$ to the angles perpendicular to the cross section. The loss function L is minimised using a Gradient descent algorithm (BFGS Quasi-newton) to compute the partial derivative of the nodes' displacement $\left(\|x_{i_{inf}} - x_{i_{tar}}\|\right)$, with $x_i = (x_i, y_i, z_i)$; then the gradient descent adjust the coordinates to match the distances to those of the sensor readings.

Figure 9a shows the virtual sleeve at rest on a cylinder after the optimisation of the sensors' readings. Figure 9b shows the configuration of the sensors used on the sleeve, highlighting the different angles measured with the inter-ring (green) and the intra-ring (cian) bend sensors.

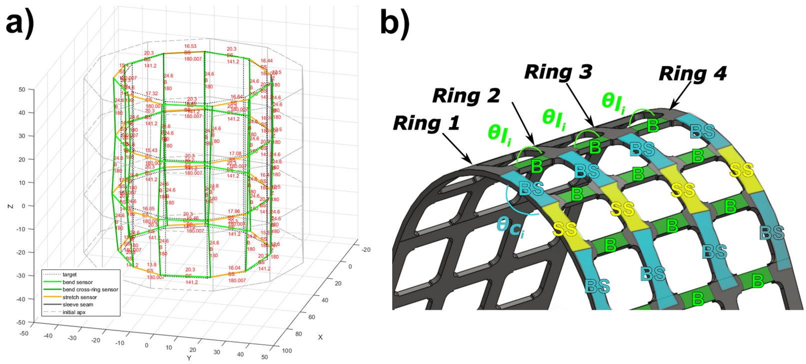

Fig. 9. a) Virtual sleeve representing the real sleeve at rest position b) Angles between sleeve edges that are being measured (Color figure online)

Noise and Error Correction. In the experiments conducted with the sleeve the data from the sensors were not always consistent and some were not producing usable results. The filtering applied to these values shifted the reconstructed shapes further than the reality. Noise and error is also produced from shape areas where interpolation or smoothing is used in between the sleeve nodes. MATLAB point cloud toolbox was used to measure this error. A combination of Iterative Closest Point and Coherent Point Drift methods were used to register the target and the optimised point clouds.

4 Results and Discussion

The developed prototypes were tested by putting them on a set of 3D printed parts with different cross sections that tests the capability of the bending and stretching of the sensors. The data obtained from these measurements was used to create the target shapes for the inference algorithm. The parts were designed in a CAD software and exported to STL to be printed. The same STL were imported into MATLAB to be used as the target shape in the inference simulation.

4.1 Textile Sleeve Evaluation

An important part of the sensors is the calibration to determine the correlation between strain/bend and change in resistance. The calibration was done with an initial state of the sleeve as a cylinder with a diameter equal to that its inner diameter without stretching the sensors. Then, the sleeves were put on cylinders with different diameters from 58 mm to 64 mm. The change in resistance ${}^{\Delta R}/_{R_0}$ was calculated for every diameter, where ΔR is the change in resistance when the sleeve is at rests (R_0) to the resistance when is on the cylinder. An initial measurement was taken at rest, then another after 10 min of being on the shapes to calculate ΔR. This procedure was performed up to 3 times for each cylinder.

Cylinders were designed in CAD and 3D printed to determine the capacity of the sleeve to measure shapes with complex round topologies on both parallel sides and cross sections. These shapes were designed in Solidworks, exported as STL for simulation and for 3D printing. Each shape have different topologies with round features that ranges from one to three different diameters in the cross sectional area, to bumps and bends on the parallel sides, as shown in Fig. 10. A cylinder with a double ellipsis was designed to test different radius on the cross section. Similarly, a cone, a double ellipsis bent cylinder, and a cone with a bump were designed to measure changes on the cross sections and on the parallel sides with different radii.

The first prototype was under constrained, limited only to detect changes in lengths. Therefore, only cylindrical and conical shapes could be measured [12]. As the sensors had a long recovery time, the sleeve was on rest and the resistance values were obtained after 10 min, then was put on the shape to calibrate/measure and another measurement was taken after 10 min, but the sensors were left to recover 24 h after put them on a greater cylinder. This is because the recovery of the sensors after stretched to 50% is ≈3.1 h.

Table 1. Main features of the developed prototypes.

Material	Contact method	Sensors configuration	Drawback	Failure	Accuracy
Off-the-shelf sensors	Copper wire	64 Stretch sensors	long recovery time (≈3.5 h), reconstruction only of cylinders and cones	NA	0.4 mm
CBE	Copper wire	8 Stretch and bend sensors	Bend sensors affected by strain, calibration not completed	Loose contacts after 15 cycles	NA
CBE	Filament wire	8 Stretch and bend sensors	Bend sensors affected by strain, calibration not completed	Loose contacts after 40 cycles	NA
CBE	Filament wire	8 Stretch and bend sensors	Calibration not completed	Loose contacts after 300 cycles	NA
CBE	Filament wire	70 Stretch and bend sensors	Calibration not completed for inter-ring sensors	Loose contacts after 300 cycles	0.08 mm
CBE	Silver coated thread	70 Stretch and bend sensors	NA	NA	NA

CBE = Carbon Black-Ecoflex polymer. NA = No Available.

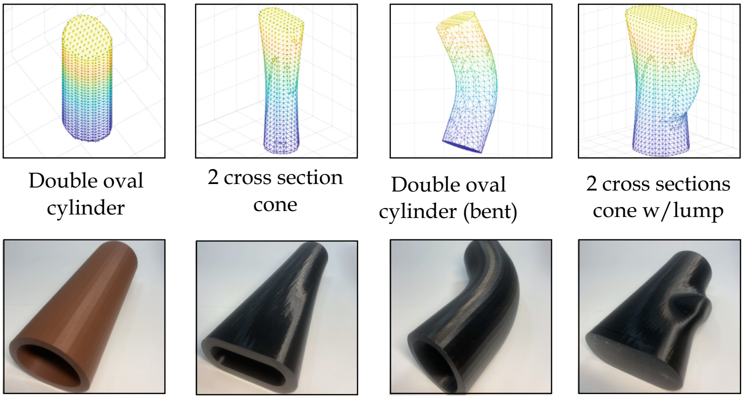

Fig. 10. Geometries used for testing the capacity of the sleeve to reconstruct complex shapes.

In the case of the second prototype, the material showed a better recovery time, 15 min, with a maximum stretchability up to 700%. However, for this iteration the contacts became loose after five calibration cycles. This was the result of the difference between the stiffness of the copper wires and the stiffness of the CE, as well as the poor surface adhesion between both components [10]. This failure was observed as an increase in resistance at rest up to 10 times.

The third prototype lasted up to 40 cycles, but the sensors rendered ineffective after this. In the case of the fourth prototype, the sensors showed a better performance for strain and bend, and the sleeve managed to withstand the calibration process of the rings. However, because of the complex configuration of the sensors, the calibration of the inter-ring bend sensors was not achieved. Moreover, when taking measurements of the complex shapes, the sensors stretched substantially more in places with features like bumps or large diameters, causing the contacts to become loose. This resulted in high resistance values of the sensors when put on the shapes to be measured. The fifth prototype is ongoing with the contacts fixed using nylon thread coated with silver. Table 1 list the main features as well as the main drawbacks and failures of each prototype.

4.2 Textile Sleeve STL Results

The work performed on the textile prototypes was mainly calibration as a result of the failure of the contacts. Despite of this, the prototype one (Sect. 2.1) and prototype four (Sect. 2.4) were used to measure features on 3D printed parts described in Sect. 4.1.

The first sleeve (Sect. 2.1) was underconstrained, therefore it could be only used to with cylinders with circular cross sections. The sleeve was used to measure the diameters of two different cones with an average difference of 0.44 ± 0.22 mm. But the results shade light on how to improve the model to add more constrains to improve the shape sensing system. The prototype four (Sect. 2.4) was used to measure geometries with more complex topologies. Although the inter-ring bend sensors provided no data because of calibration issues, the data of the intra-ring bend and strain sensors was used for the reconstruction. From the topology of the sleeve sensors, the bending of the stretch sensors had to be assumed, and the principle used to assign angles was the fact that the sum of all 11 angles around each ring computes to 360°. Outlier data from the working bend sensors due to loose contacts were also filtered out, and replaced with the adjacent bend sensor of the neighbouring ring. Figure 11 depicts the selected shapes from the previous section, as reconstructed by the optimisation algorithm. The similarities with the target shape are difficult to distinguish due to lack of or interpolated angular data.

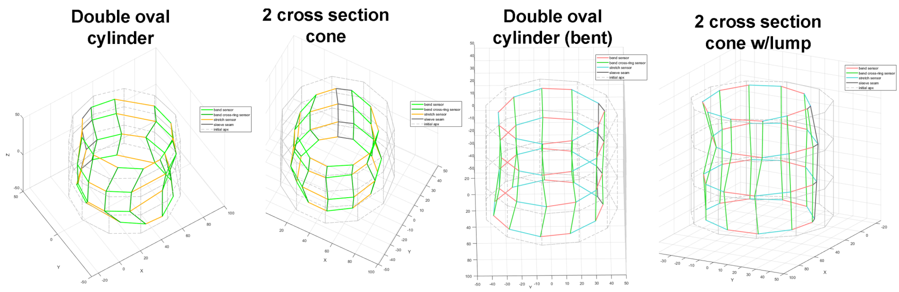

Fig. 11. Real sleeve data from prototype 4. Bend sensors are in green and red, stretch sensors in yellow or cyan, and the sleeve's seam is in grey. (Color figure online)

4.3 Virtual Sleeve on Leg Model Results

Figure 12 Shows the simulation of a leg model with a sleeve with higher number of rings and nodes. The challenge presented is draping the sleeve over the ankle and draping a 90° bend.

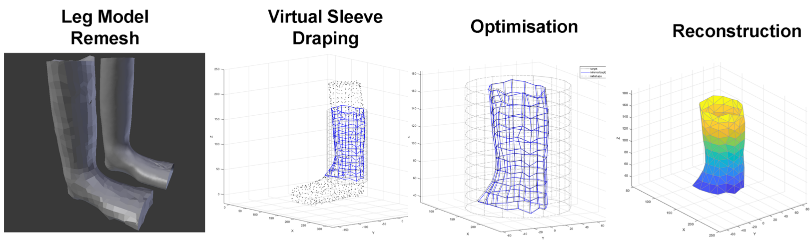

Fig. 12. Simulated reconstruction of a leg model using a 11-ring with 16 sensor nodes per ring virtual sleeve.

5 Recommendations for Smart Textiles for Body-Shape Sensing

The main limitation to address in the current research was the interfacing of the sensors, therefore a good method that prevents the sensors from becoming inoperative is needed. As it has been demonstrated, although thread has a better surface adhesion to conductive elastomer, its feasibility still to be proved. If successful, this will increase the life span of the sensors and their reliability. Similarly, the developed prototypes are structured arrays of sensors with a defined topology. In order to have better results, the arrangement of sensors has to be explored. The possibility of changing the bend/stretch sensor's order in each ring should be explored so that each intra-ring bend sensor has a stretch sensor adjacent to it on the neighbouring ring. This gives the potential to provide better results when the algorithm estimates the bending of the stretch sensors. Deploying stretch sensors in the ring cross section will also provide more data for the inference process. Similarly, an unstructured mesh of sensors to cover a higher surface area with less elements. Another possibility will be the capability of measure both strain and bend with a single structure.

6 Conclusions and Future Work

This paper has presented lessons learned fro work in progress of a shape sensing technology as means for creating a smart textile with stretchable and bendable soft sensors. Five different prototypes and the main characteristics and failures of each one were presented. Similarly, challenges in the shape inference process and algorithm for anticipating missing or erroneous data have also been presented and discussed. Future work will look for the improvement of the system by addressing the issues here presented for each prototype and to explore the feasibility of capacitive sensors.

Acknowledgement. This work was funded by EPSRC, GCRF, and NIHR. Contact number: EP/R013837/1 (SmartSensOtics).

References

1. Barrios-Muriel, J., Romero-Sánchez, F., Alonso-Sánchez, F.J., Rodríguez Salgado, D.: Advances in orthotic and prosthetic manufacturing: a technology review. Materials **13**(2) (2020). https://doi.org/10.3390/ma13020295. https://www.mdpi.com/1996-1944/13/2/295
2. Bello, H., Zhou, B., Suh, S., Lukowicz, P.: MoCapaci: posture and gesture detection in loose garments using textile cables as capacitive antennas. In: 2021 International Symposium on Wearable Computers. ACM (2021). https://doi.org/10.1145/3460421.3480418

3. Costa, J.C., Spina, F., Lugoda, P., Garcia-Garcia, L., Roggen, D., Münzenrieder, N.: Flexible sensors–from materials to applications. Technologies **7**(2), 35 (2019). https://doi.org/10.3390/technologies7020035
4. Dunne, L.E., Walsh, P., Hermann, S., Smyth, B., Caulfield, B.: Wearable monitoring of seated spinal posture. IEEE Trans. Biomed. Circuits Syst. **2**(2), 97–105 (2008). https://doi.org/10.1109/tbcas.2008.927246
5. Farhan, M., Wang, J.Z., Bray, P., Burns, J., Cheng, T.L.: Comparison of 3D scanning versus traditional methods of capturing foot and ankle morphology for the fabrication of orthoses: a systematic review. J. Foot Ankle Res. **14**(1), 1–11 (2021). https://doi.org/10.1186/s13047-020-00442-8
6. Garcia-Garcia, L.A., Rodriguez-Salvador, M.: Additive manufacturing knowledge incursion on orthopaedic device: the case of hand orthoses. In: Proceedings of the 3rd International Conference on Progress in Additive Manufacturing, (Pro-AM 2018), pp. p571–6 (2018)
7. García-García, L.A., Rodríguez-Salvador, M., Moya-Bencomo, M.D.: Development of a customized wrist orthosis for flexion and extension treatment using reverse engineering and 3D printing. In: Lhotska, L., Sukupova, L., Lacković, I., Ibbott, G.S. (eds.) World Congress on Medical Physics and Biomedical Engineering 2018. IP, vol. 68/2, pp. 609–613. Springer, Singapore (2019). https://doi.org/10.1007/978-981-10-9038-7_113
8. Garcia-Garcia, L.A., Valsamakis, G., Kreitmair, P., Munzenrieder, N., Roggen, D.: Inferring complex textile shape from an integrated carbon black-infused ecoflex-based bend and stretch sensor array. In: Adjunct Proceedings of the 2021 ACM International Joint Conference on Pervasive and Ubiquitous Computing and Proceedings of the 2021 ACM International Symposium on Wearable Computers, UbiComp '21, pp. 298–303. Association for Computing Machinery, New York (2021). https://doi.org/10.1145/3460418.3479347
9. García-Patiño, A., Khoshnam, M., Menon, C.: Wearable device to monitor back movements using an inductive textile sensor **20**(3), 905 (2020). https://doi.org/10.3390/s20030905
10. García-García, L.A., Costa, J.C., Lugoda, P., Roggen, D., Münzenrieder, N.: Copper wire based electrical contacts for direct interfacing of stretchable sensors. In: 2020 IEEE SENSORS, pp. 1–4. IEEE (2020). https://doi.org/10.1109/SENSORS47125.2020.9278749
11. Lou, M., et al.: Highly wearable, breathable, and washable sensing textile for human motion and pulse monitoring **12**(17), 19965–19973 (2020). https://doi.org/10.1021/acsami.0c03670
12. Lugoda, P., Garcia-Garcia, L.A., Richoz, S., Munzenrieder, N., Roggen, D.: ShapeSense3d. ACM (2019). https://doi.org/10.1145/3341162.3343846
13. Mattmann, C., Amft, O., Harms, H., Troster, G., Clemens, F.: Recognizing upper body postures using textile strain sensors. In: 2007 11th IEEE International Symposium on Wearable Computers, pp. 29–36 (2007). https://doi.org/10.1109/ISWC.2007.4373773
14. Tormene, P., et al.: Estimation of human trunk movements by wearable strain sensors and improvement of sensor's placement on intelligent biomedical clothes. Biomed. Eng. Online **11**(1), 1–8 (2012). https://doi.org/10.1186/1475-925x-11-95
15. Wang, Y., Tan, Q., Pu, F., Boone, D., Zhang, M.: A review of the application of additive manufacturing in prosthetic and orthotic clinics from a biomechanical perspective. Engineering **6**(11), 1258–1266 (2020). https://doi.org/10.1016/j.eng.2020.07.019. https://www.sciencedirect.com/science/article/pii/S2095809920302575

16. Yapici, M.K., Alkhidir, T., Samad, Y.A., Liao, K.: Graphene-clad textile electrodes for electrocardiogram monitoring. Sensors Actuators B: Chem. **221**, 1469–1474 (2015). https://doi.org/10.1016/j.snb.2015.07.111
17. Zaltieri, M., et al.: A wearable device based on a fiber bragg grating sensor for low back movements monitoring **20**(14), 3825 (2020). https://doi.org/10.3390/s20143825